Climatic Impact of Global-Scale Deforestation: Radiative versus Nonradiative Processes

Edouard Davin, Nathalie de Noblet-Ducoudré

Climatic Impact of Global-Scale Deforestation: Radiative versus Nonradiative Processes

EDOUARD L. DAVIN* AND NATHALIE DE NOBLET-DUCOUDRÉ

Le Laboratoire des Sciences du Climat et l'Environnement, L'Institut Pierre-Simon Laplace (UMR CEA–CNRS–l'Université de Versailles Saint-Quentin-en-Yvelines), Gif-sur-Yvette, France

(Manuscript received 23 February 2009, in final form 30 July 2009)

ABSTRACT

A fully coupled land–ocean–atmosphere GCM is used to explore the biogeophysical impact of large-scale deforestation on surface climate. By analyzing the model sensitivity to global-scale replacement of forests by grassland, it is shown that the surface albedo increase owing to deforestation has a cooling effect of −1.36 K globally. On the other hand, forest removal decreases evapotranspiration efficiency and decreases surface roughness, both leading to a global surface warming of 0.24 and 0.29 K, respectively. The net biogeophysical impact of deforestation results from the competition between these effects. Globally, the albedo effect is dominant because of its wider-scale impact, and the net biogeophysical impact of deforestation is thus a cooling of −1 K. Over land, the balance between the different processes varies with latitude. In temperate and boreal zones of the Northern Hemisphere the albedo effect is stronger and deforestation thus induces a cooling. Conversely, in the tropics the net impact of deforestation is a warming, because evapotranspiration efficiency and surface roughness provide the dominant influence. The authors also explore the importance of the ocean coupling in shaping the climate response to deforestation. First, the temperature over ocean responds to the land cover perturbation. Second, even the temperature change over land is greatly affected by the ocean coupling. By assuming fixed oceanic conditions, the net effect of deforestation, averaged over all land areas, is a warming, whereas taking into account the coupling with the ocean leads, on the contrary, to a net land cooling. Furthermore, it is shown that the main parameter involved in the coupling with the ocean is surface albedo. Indeed, a change in albedo modifies temperature and humidity in the whole troposphere, thus enabling the initially land-confined perturbation to be transferred to the ocean. Finally, the radiative forcing framework is discussed in the context of land cover change impact on climate. The experiments herein illustrate that deforestation triggers two opposite types of forcing mechanisms—radiative forcing (owing to surface albedo change) and nonradiative forcing (owing to change in evapotranspiration efficiency and surface roughness)—that exhibit a similar magnitude globally. However, when applying the radiative forcing concept, nonradiative processes are ignored, which may lead to a misrepresentation of land cover change impact on climate.

1. Introduction

Land cover change can affect climate conditions through both biogeochemical and biogeophysical processes. This study focuses on the biogeophysical effect of land cover change, arising from changes in the physical properties of the land surface. Exchanges of radiation, water, heat, and momentum between the land and the atmosphere are mediated by plants. Therefore, changes in the vegetation cover can perturb these fluxes and hence impact the climate.

Already 15%–30% of the natural forest cover has been converted to pasture or cropland (Goldewijk 2001). Historically, the largest part of this conversion affected temperate forests in Eurasia and North America (Ramankutty and Foley 1999; Goldewijk 2001). Over the last decades, however, the rate of deforestation strongly accelerated in tropical regions and it is projected that a large part of the tropical forest will be lost by the end of the twenty-first century (Alcamo et al. 1994). Yet the biogeophysical effect of these conversions is usually not included in projections of future climate change. For instance, among

* Current affiliation: Institute for Atmospheric and Climate Science, ETH Zurich, Zurich, Switzerland.

Corresponding author address: Edouard Davin, Institute for Atmospheric and Climate Science, ETH Zurich, Universitätstrasse 16, 8092 Zurich, Switzerland.
E-mail: edouard.davin@env.ethz.ch

DOI: 10.1175/2009JCLI3102.1

the 23 climate models that participated in the Fourth Assessment Report (AR4) of the Intergovernmental Panel on Climate Change (IPCC), only three of them included a transient land use forcing over the twentieth and twenty-first centuries (Solomon et al. 2007). Moreover, afforestation or reforestation have been proposed as a strategy to mitigate climate change, but the climate benefit of such policies is still evaluated in terms of carbon sequestration potential without considering biogeophysical implications (Nabuurs et al. 2007). There is thus a growing need to advance our understanding of the biogeophysical impact of land cover change, first to improve projections of climate change trajectory and second to address more exhaustively the potential of afforestation or reforestation to mitigate climate change.

Indications that land cover change can affect global or regional climate through biogeophysical processes have been progressively gained from various studies using climate model simulations. Historical deforestation at midlatitudes may have cooled Northern Hemisphere climate (e.g., Brovkin et al. 1999; Bonan 1997; Betts 2001; Govindasamy et al. 2001; Bounoua et al. 2002; Feddema et al. 2005b; Brovkin et al. 2006) because of the associated increase in surface albedo. On the other hand, it is suggested that possible future removal of tropical forests could lead to a locally warmer and drier climate (e.g., Dickinson and Henderson-Sellers 1988; Lean and Warrilow 1989; Nobre et al. 1991; Henderson-Sellers et al. 1993; Lean and Rowntree 1997; DeFries et al. 2002; Feddema et al. 2005a) because of reduced evapotranspiration rates. In light of these two types of experiments one can see the emergence of a paradox: deforestation at different latitudes may have a different impact. This paradox becomes even more apparent in more conceptual experiments contrasting the impact of deforestation in different range of latitudes (Claussen et al. 2001; Snyder et al. 2004; Gibbard et al. 2005; Bala et al. 2007). For instance, Claussen et al. (2001) used a climate system model of intermediate complexity to investigate the biogeophysical impact of a complete deforestation in the belt 50°–60°N and alternatively in the belt 10°S–0°. They found that boreal deforestation leads to a surface cooling, while, on the contrary, tropical deforestation produces a warming of the deforested region and a slight cooling elsewhere. It has been suggested that change in radiation (through change in surface albedo) is the dominant influence at high latitudes, while the hydrological cycle (i.e., change in evapotranspiration rates) plays a more prominent role in the tropics (Claussen et al. 2001; Pielke et al. 2002; Bala et al. 2007; Betts et al. 2007; Bonan 2008). However, the relative importance of these different processes has never been quantified, thus preventing a comprehensive understanding of the overall biogeophysical effect of deforestation at different latitudes.

Therefore, the main goal of this study is to assess the role of individual processes (i.e., change in surface albedo, evapotranspiration efficiency, and surface roughness) in shaping the global and local biogeophysical impact of deforestation, with emphasis on surface temperature. We compare the climate of a maximally forested world with the climate of a completely deforested world, where trees are replaced by grasses. This extreme scenario does not aim to represent a realistic land cover perturbation; instead it allows us to compare the effect of deforestation at different locations with homogeneous deforestation rates. While statistical significance is often an issue when analyzing land cover change experiments, such a large perturbation also offers the advantage of obtaining a signal that largely overtakes internal variability. To quantify the relative importance of the individual factors involved in the net biogeophysical effect of deforestation, we perform additional experiments in which those factors are considered separately.

Furthermore, most of the previous land cover change experiments have been using climate models of intermediate complexity or atmospheric models without explicit representation of the ocean. In this study we use a fully coupled land–ocean–atmosphere GCM that enables us to address the impact of deforestation in a more comprehensive manner. In particular, we investigate how the climate sensitivity to deforestation is influenced by ocean–atmosphere coupling.

2. Model and experiments

We use the Institut Pierre-Simon Laplace (IPSL) climate model (Marti et al. 2005), which couples the Laboratoire de Météorologie Dynamique (LMDZ4) atmospheric GCM (Hourdin et al. 2006) with the Océan Parallélisé (OPA) ocean GCM (Madec et al. 1998), the Louvain-la-Neuve Sea Ice Model (LIM; Fichefet and Maqueda 1997), and the Organizing Carbon and Hydrology in Dynamic Ecosystems (ORCHIDEE) land surface model (Krinner et al. 2005). No flux adjustments are used in the coupling of these models. The atmospheric model is run at a resolution of $3.75° \times 2.5°$ with 19 vertical levels in the atmosphere. The ocean has 31 vertical levels and a horizontal resolution of about 2° with higher latitudinal resolution of roughly 0.5° in the equatorial ocean. The ORCHIDEE land surface scheme describes both biogeophysical and biogeochemical processes in the biosphere. The vegetation phenology is not prescribed and leaf area index (LAI) is computed, for each of the 12 plant functional types (PFT) distinguished by ORCHIDEE, from photosynthetic activity and carbon allocation to the

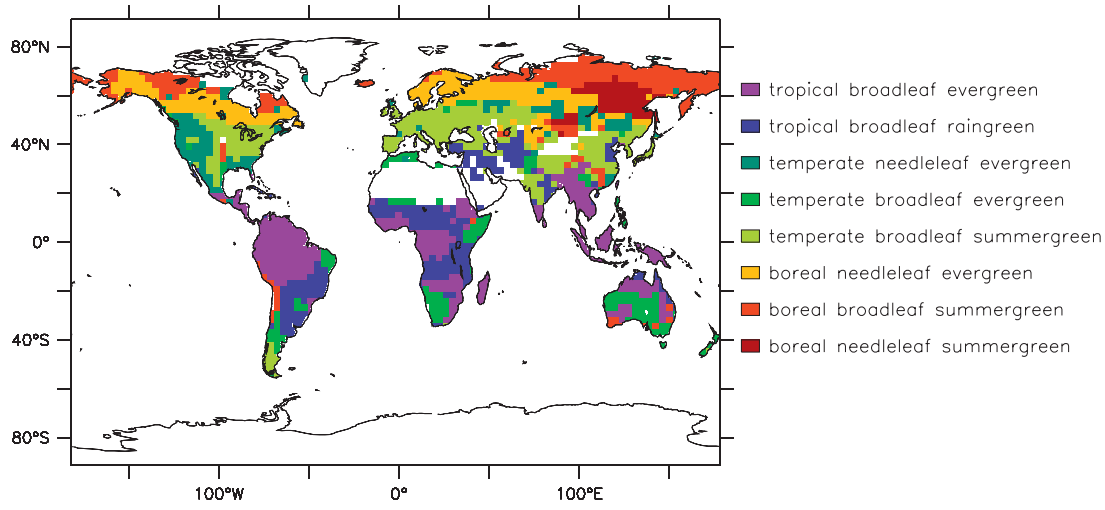

FIG. 1. Land cover map prescribed in simulation FOREST.

vegetation compartments. The LAI is then used for the calculation of key variables such as surface albedo, surface roughness, and canopy conductance.

To evaluate the impact of global-scale deforestation we contrast a maximally forested world and a completely deforested world. The vegetation map representing the maximally forested world (Fig. 1) was constructed by modifying the standard present-day land cover map used by ORCHIDEE (Loveland et al. 2000). For each grid cell the dominant tree type in the present-day map was expanded so that it occupied 100% of the grid cell. In grid cells where no tree type is present in the map, we used the tree type found in the nearest grid cell. Grid points having more than 80% of bare soil were kept unchanged and the fraction of glaciers was not changed too. This was done to avoid placing forests in desert regions where they would not be able to maintain realistic productivity and leaf area. For the vegetation map representing the deforested world, we simply replaced the trees present in the first map by grassland. The partitioning of grass into C3 and C4 types was done by examining the climatic envelop that is more appropriate to C3 or C4 plants as defined within the Lund Postdam Jena (LPJ) model (Sitch et al. 2003).

We then perform two experiments with the IPSL model. In the first experiment (referred to as FOREST) the land cover map representing the forested world is prescribed. The second experiment (referred to as GRASS) uses the land cover map representing the completely deforested world.

To help understand the physical mechanisms behind the overall climate response to deforestation, we perform three additional experiments in which we only consider the effect owing to surface albedo (simulation ALB), surface roughness (simulation RGH), and evapotranspiration efficiency (simulation EVA), respectively. The experimental design for these simulations is as follows. Simulation ALB has the same setup as simulation FOREST except for the surface albedo calculation, which assumes a grass cover. Similarly, simulation RGH has the same setup as simulation FOREST except for the surface roughness calculation, which assumes a grass cover. Finally, for simulation EVA a slightly different strategy was used since it is not straightforward to perturb directly the relevant parameters. Indeed, evapotranspiration efficiency, which represents the ability of the vegetation to transfer water from the soil to the atmosphere, involves various parameters (e.g., rooting depth, canopy water holding capacity, photosynthesis, and stomatal conductance); most of them calculated dynamically in the model. Therefore, we isolate this effect indirectly by acting on both surface albedo and surface roughness calculations. Simulation EVA has thus the same setup as simulation GRASS, except that the surface albedo and surface roughness calculations assume a forest cover. This way the albedo and roughness characteristics in simulation EVA are consistent with a forest cover, while the rest (which we define as evapotranspiration efficiency) is consistent with a grass cover. (Note that change in evapotranspiration can already occur through changes in surface albedo or surface roughness, meaning that the pure hydrological effect of deforestation, which simulation EVA isolates, is only related to change in the partitioning between evapotranspiration and sensible heat flux.)

All simulations were initialized from an existing preindustrial control run and have constant greenhouse gas (GHG) concentrations fixed at preindustrial values. To let the model reach a quasi-equilibrium state we run all simulations for 60 years and we then run 50 additional

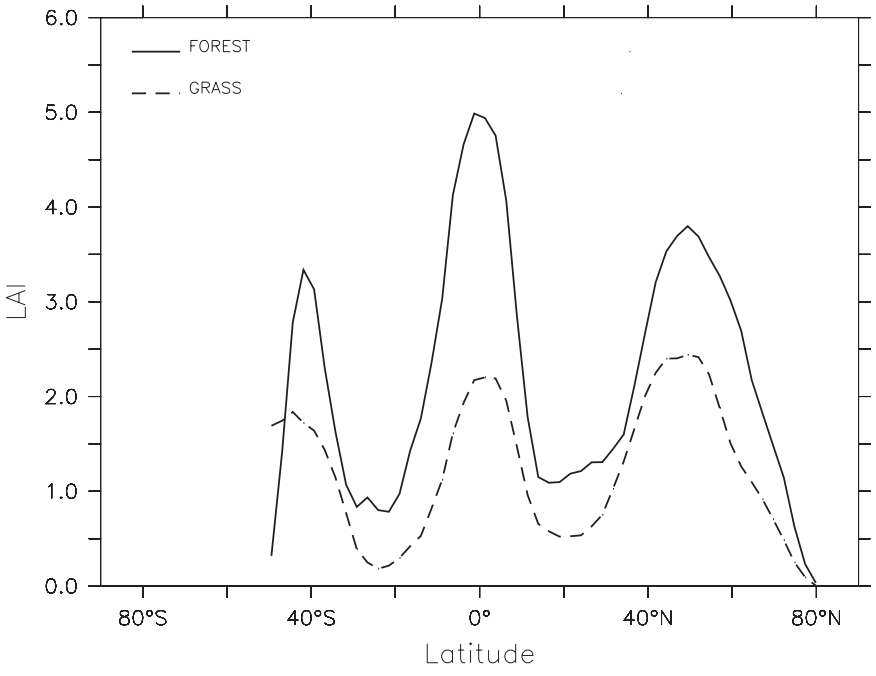

FIG. 2. Zonally averaged summer (JJA) LAI for simulations FOREST and GRASS.

years used for analysis. Over the period of analysis all the simulations are fairly stable. For instance, simulation FOREST has a global temperature drift of only 0.04 K over the last 50 years.

3. Results

a. Overall biogeophysical impact of deforestation

To give a feeling of the importance of the land cover perturbation imposed in our experiments, we examine the change in LAI, which is a key variable influencing radiation fluxes, water exchanges, and aerodynamic properties of the boundary layer. Figure 2 compares the summer LAI simulated in experiment FOREST and in experiment GRASS. Generally, LAI is higher in temperate and tropical regions compared to the subtropics (where vegetation is sparser and less productive). The LAI decreases at every latitude when forest is replaced by grassland. This decrease is more drastic in the tropics where the initial LAI of the tropical forest is higher than elsewhere. Conversely, the change in LAI is limited in the subtropics where LAI is already low in the control case.

The land cover perturbation imposed in our experiments is spatially homogeneous in the sense that trees are replaced by grass everywhere on land. Despite this homogeneity, the annual mean surface temperature change in simulation GRASS compared to simulation FOREST (Fig. 3a) varies strongly across regions, in both magnitude and sign. A substantial cooling of northern high and midlatitudes as well as of most parts of the oceans follows deforestation. Poleward of 40°N, the cooling is as large as 4 K or more. On the contrary, tropical regions, in particular South America, the southern part of Africa, and South Asia, are subjected to a substantial warming. Over Amazonia, for instance, surface climate warms by about 1 K or more in response to forest removal. Globally, the net effect of deforestation is a surface cooling of 1 K, as indicated in Table 1.

Hence, one of the most striking features arising from these experiments is the strong latitudinal dependency of the climate response to deforestation. This points to the contradicting climatic role of temperate and boreal forests versus tropical forests. As stated in the introduction, this paradox also emerges from the existing literature. In that respect, our results are in line with previous findings. However, the underlying mechanisms behind this paradox are still unclear. Therefore, the goal of the analysis proposed in the next sections is to provide a basis for a better understanding of this result. Additionally, another striking result is the ocean cooling after deforestation, which will also be further investigated in the following.

b. Influence of the individual vegetation characteristics

1) SURFACE ALBEDO

The difference between simulation ALB and simulation FOREST highlights the role of albedo change when

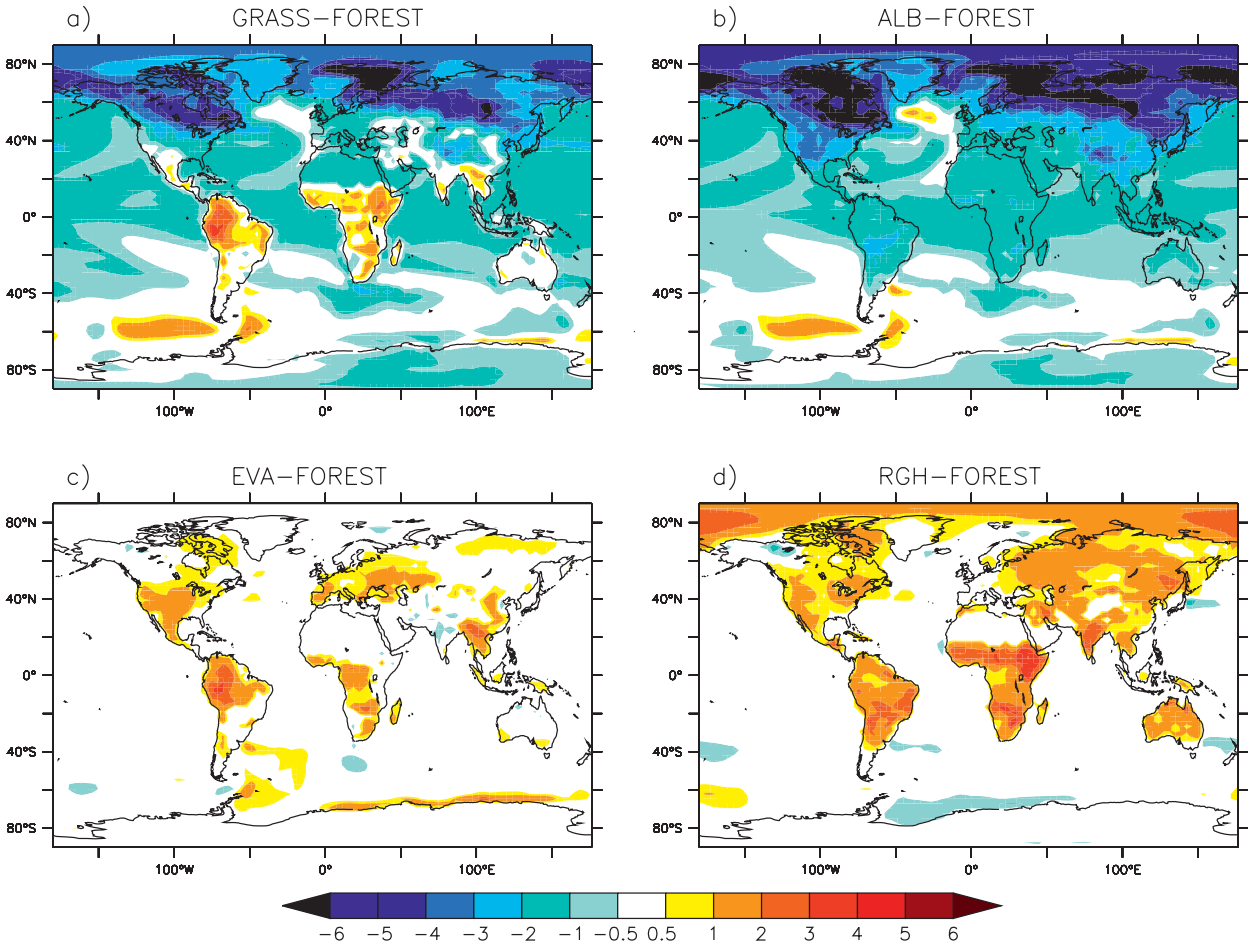

FIG. 3. Annual mean surface temperature change (K) in (a) simulation GRASS, (b) simulation ALB, (c) simulation EVA, and (d) simulation RGH, relative to simulation FOREST.

replacing forest by grass. Overall, deforestation produces a strong cooling through change in surface albedo. The annual mean global cooling in simulation ALB compared to simulation FOREST reaches 1.36 K (Table 1).

The spatial pattern of the surface temperature response (Fig. 3b) shows a stronger cooling at northern high latitudes (above 4 K) compared to low latitudes (cooling around 1 K). This ''polar amplification'' pattern is a classical feature also arising from GHG-induced climate change (Solomon et al. 2007) and reflecting the existence of stronger positive feedback mechanisms near the pole. However, in the case of land cover change both the distribution of the forcing and of the feedbacks tend to enhance the response near the pole. Figure 4 shows the annual mean change in surface albedo between simulations ALB and simulation FOREST. Conversion from forest to grass leads to higher land albedo and consequently decreases absorbed solar radiation at the surface and hence temperature. In tropical regions, the change in albedo does not exceed 10%, while at northern mid- and high latitudes changes are much more pronounced. This relates to the fact that the albedo difference between trees and grassland is magnified by the presence of snow (e.g., Betts 2000, 2001). Additionally, the initial albedo increase is further amplified in these regions by the snow–albedo feedback with snow being more abundant and persistent under colder conditions.

Furthermore, it is interesting to note that the surface cooling is transferred to the ocean, even though the

TABLE 1. Annual mean change in surface temperature (ΔT_s) and in net radiation at the top of the atmosphere (ΔR) in the different simulations with respect to simulation FOREST. Changes in net radiation are averaged over the first 10 years of simulation.

	ΔT_s K	ΔR W m^{-2}
GRASS-FOREST	−1.00	−1.07
ALB-FOREST	−1.36	−1.27
EVA-FOREST	0.24	0.02
RGH-FOREST	0.29	0.04

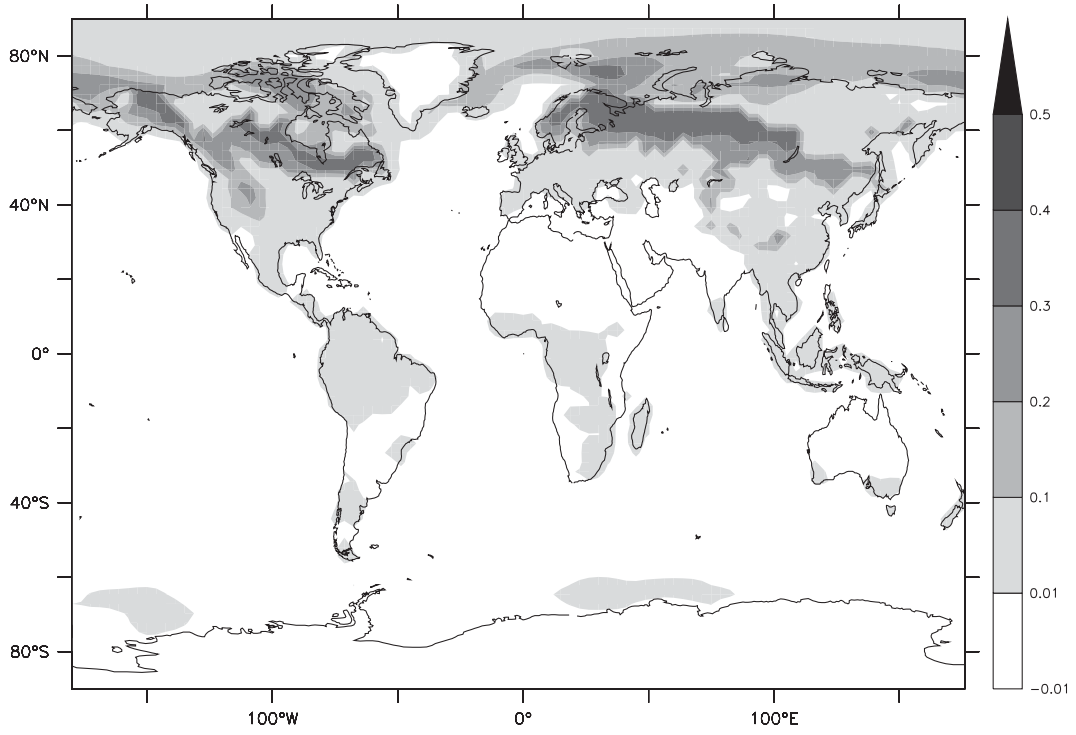

FIG. 4. Annual mean surface albedo change in simulation ALB relative to simulation FOREST.

albedo perturbation occurs only on land. This result will be further discussed in section 3d.

2) EVAPORATION EFFICIENCY

The effect of deforestation through change in evaporation efficiency is emphasized in simulation EVA. Globally, we find that this effect increases surface temperature by 0.24 K in simulation EVA compared to simulation FOREST (Table 1). Compared to the albedo effect, the evapotranspiration efficiency effect is thus of opposite sign.

The geographical distribution of the annual mean surface temperature change is shown in Fig. 3c. The surface warming is around 1 K in North America and the western part of Eurasia. It is well above 1 K in tropical regions such as Amazonia, the south part of Africa, and Southeast Asia. The temperature response exhibits no polar amplification pattern and no remote impact on oceanic regions.

Compared to grass, trees are generally more efficient in transferring water from the soil to the atmosphere because of their deeper roots and larger leaf area. For a given amount of solar energy available at the surface, forest thus tends to maintain a cooler surface temperature by releasing more energy in the form of latent heat. Hence, conversion from forest to grass tends to warm the surface through this effect. To illustrate this mechanism and its seasonality, Fig. 5 presents the surface temperature anomaly and the associated change in evapotranspiration for winter [December–February (DJF)] and summer [June–August (JJA)]. For both seasons, the distribution of positive temperature anomalies is well correlated with lower evapotranspiration rates. The rationale of this correlation is that the reduction in evapotranspiration has to be compensated by an increase in surface temperature and sensible heat. In some locations, especially in Siberia during summer, the surface temperature rise cannot be directly attributed to evapotranspiration change but is more likely due to the amplification of the initial warming by the snow–albedo feedback. In the tropics, the evapotranspiration decrease and thus temperature rise are larger during the dry season (DJF for north Amazonia, West Africa, and Southeast Asia; JJA for south Amazonia and South Africa). This result is in line with site measurements in south Amazonia, indicating that the largest evapotranspiration difference between forest and grassland occurs during the dry season (von Randow et al. 2004). Indeed, during dry conditions, trees can maintain a large uptake of water thanks to their deep roots, while grasses are more strongly subjected to water limitation. Temperate regions (mainly North America and Europe) are affected almost exclusively in summer, with evapotranspiration being strongly reduced and temperature being increased. There is not

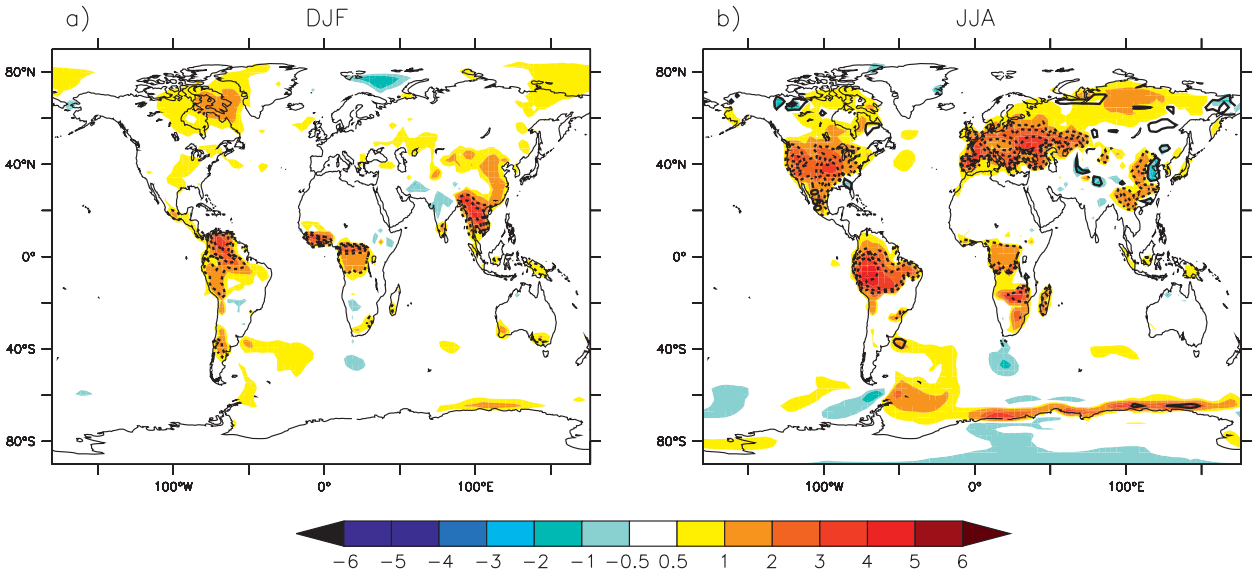

FIG. 5. Change in surface temperature (K) and in evapotranspiration (contours every 0.5 mm day^{-1}, with dashed line for negative values) in simulation EVA compared to simulation FOREST for (a) DJF and (b) JJA.

such effect in winter since evapotranspiration is weak during this season and since summer green trees shed their leaves so that they cannot transpire more than grass.

3) SURFACE ROUGHNESS

Possible impact of land cover change on climate through change in surface roughness is largely unknown. Conversion from forest to grassland tends to reduce the roughness of the landscape and thus to reduce the turbulence in the boundary layer. However, it is not trivial to predict conceptually the effect that this reduction may have on surface temperature. Indeed, the reduction of heat and water vapor transport associated with reduced turbulence may be compensated by greater gradients of humidity and temperature between the surface and the atmosphere (Sud et al. 1988).

We find that change in surface roughness, emphasized in simulation RGH, warms the surface by 0.29 K globally (Table 1). Figure 3d indicates that this surface warming is around 1 K over most land areas and is even more pronounced in the tropics. Change in surface roughness has thus a similar effect than change in evapotranspiration efficiency, characterized by a surface warming restricted to land.

To understand the mechanism behind this effect we further examine the seasonality of the change in roughness, surface fluxes, and temperature. The change in surface roughness for winter and summer is shown in Fig. 6. Conversion from forest to grassland leads to lower surface roughness. This reduction is larger in the tropics because tropical forest is taller and has a larger LAI than other forests. Moreover, the reduction in surface roughness is almost constant over the year in tropical regions, whereas at higher latitudes the change is more pronounced in summer than in winter because of the larger seasonal cycle of the LAI. The surface temperature change for winter and summer is shown in Fig. 7 along with the change in turbulent fluxes (i.e., the sum of sensible heat flux and latent heat flux). It appears that there is a very tight link between the surface temperature increase and the decrease in turbulent fluxes, at least for tropical regions and also for temperate regions during summer. Indeed, reduced surface roughness leads to weaker turbulent exchanges. Since the energy available at the surface cannot be transferred to the atmosphere through turbulent fluxes, the surface tends to warm. Ultimately, surface temperature increase implies that more energy is transferred in the form of outgoing longwave radiation. This can be checked by examining the change in the radiative fluxes at the surface. Figure 8 indeed indicates an increase in outgoing longwave radiation over land at most latitudes. It can also be seen from Fig. 8 that this increase in outgoing longwave flux cannot be explained by any change in net solar radiation or in incoming longwave radiation. Instead, the change in outgoing longwave radiation is directly linked to the reduction of turbulent fluxes.

This result is consistent with observations of the surface energy balance over forest and pasture sites in Amazonia, where upward longwave radiation was found to be on average 13.2% higher over pasture because of reduced turbulent exchanges (Culf et al. 1996, their Table 10). Our results is also in line with the regional

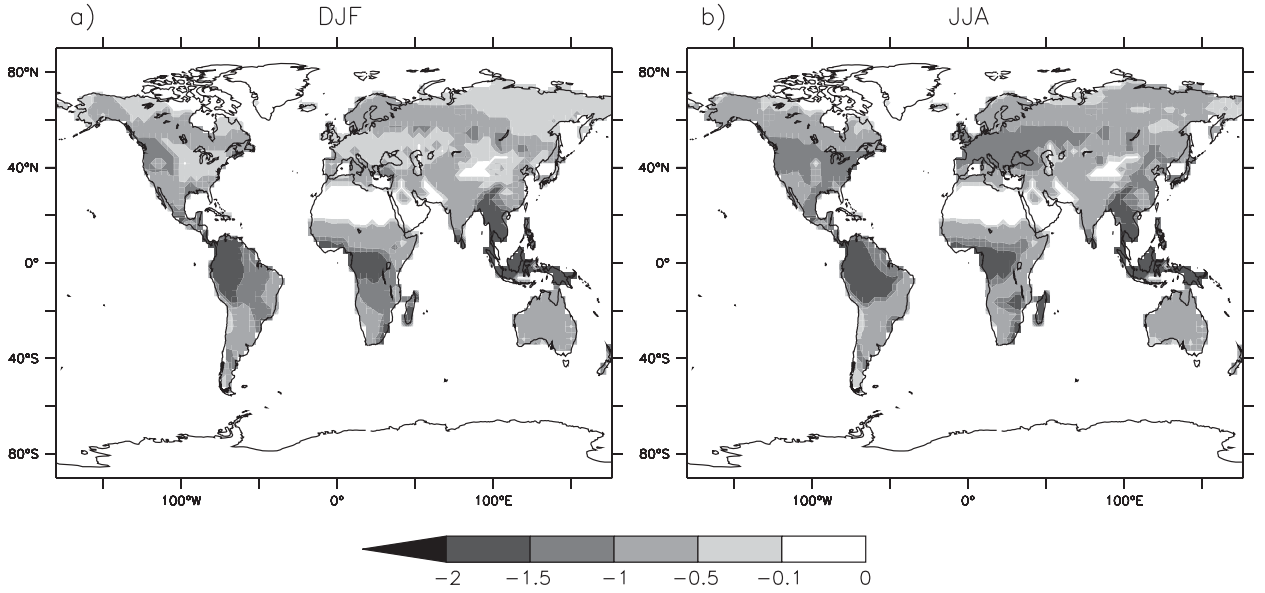

FIG. 6. Change in surface roughness length (m) in simulation RGH relative to simulation FOREST for (a) DJF and (b) JJA.

studies from Lean and Warrilow (1989) and Lean et al. (1996), who found that reduction in surface roughness owing to Amazonian deforestation has a strong warming influence in their atmospheric model.

c. *Contribution of the individual processes to the net biogeophysical effect*

The net biogeophysical effect of deforestation can be viewed as the combination of the individual effects described in the previous section. Combining these effects linearly (i.e., summing the surface temperature change due to surface albedo, evapotranspiration efficiency, and surface roughness as ALB-FOREST + EVA-FOREST + RGH-FOREST) leads to the reconstructed surface temperature change shown in Fig. 9b. Strikingly, this reconstructed signal is in strong agreement with the actual net biogeophysical effect of deforestation deduced from GRASS-FOREST (Fig. 9a). The agreement, however, is not perfect because of the existence of nonlinear interactions between the individual effects. It is possible to

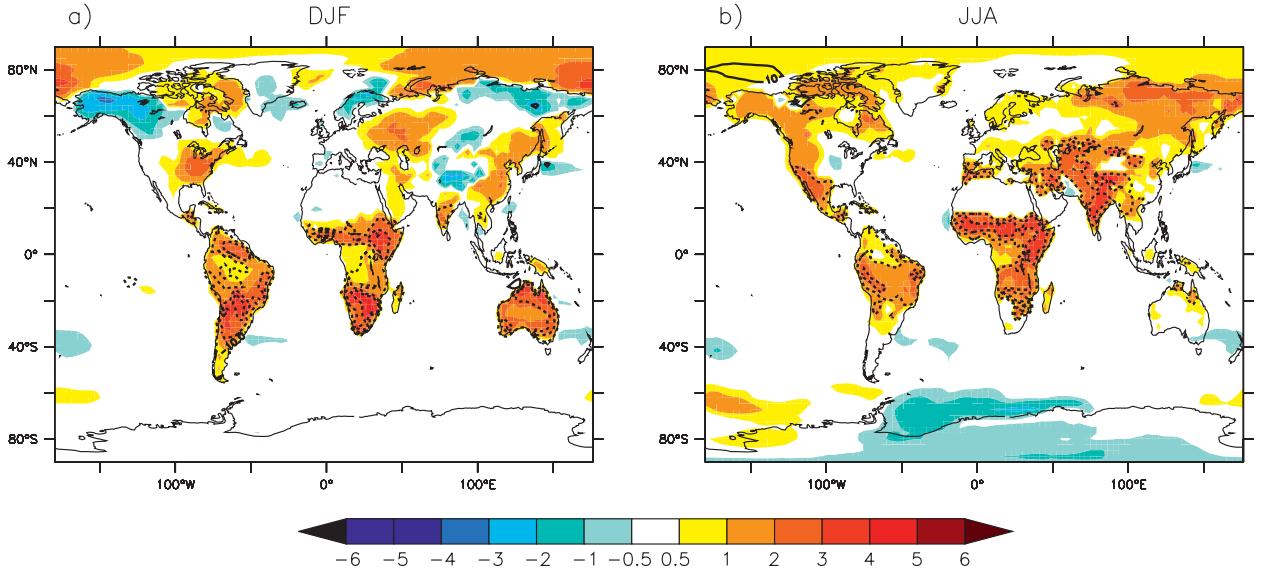

FIG. 7. Change in surface temperature (K) and in turbulent heat flux (sum of latent and sensible heat; contours every 10 W m^{-2}, with dashed line for negative values) in simulation RGH compared to simulation FOREST for (a) DJF and (b) JJA.

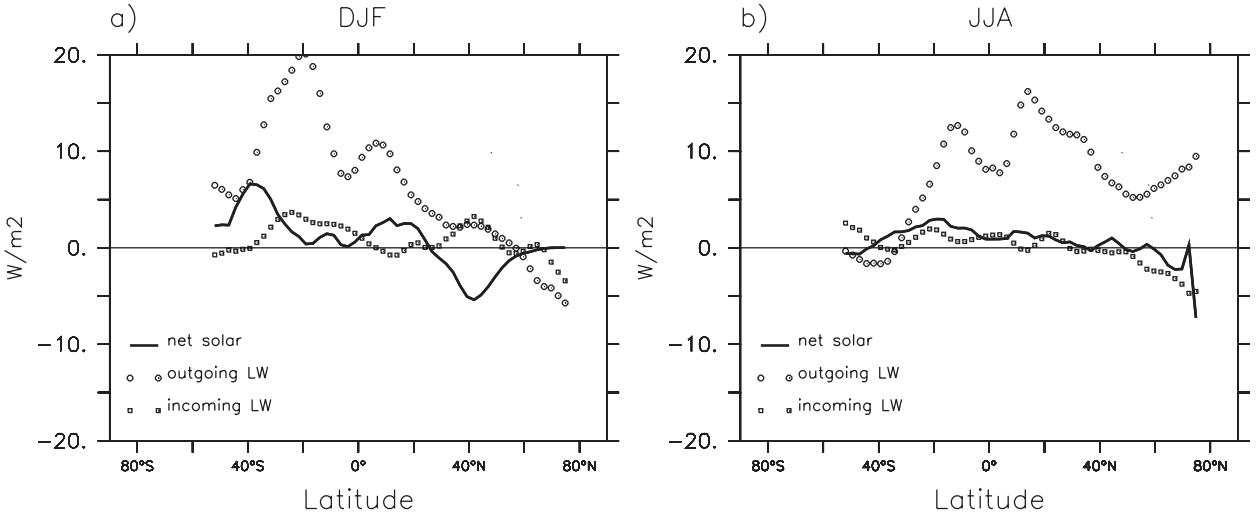

FIG. 8. Change in net solar radiation, outgoing longwave radiation, and incoming longwave radiation at the surface, in simulation RGH relative to simulation FOREST, for (a) DJF and (b) JJA. Fluxes are zonally averaged over land and considered positive when directed toward the atmosphere.

quantify this nonlinear term as the residual between the reconstructed signal and the overall net biogeophysical effect, that is, (ALB-FOREST + EVA-FOREST + RGH-FOREST) − (GRASS-FOREST).

Having now determined the complete set of factors contributing to the overall biogeophysical effect of deforestation (namely, surface albedo change, change in evapotranspiration efficiency, change in surface roughness, and nonlinear interactions between the previous processes), it becomes possible to address how much each of these factors contribute to the overall signal due to deforestation. The top panels in Figs. 10a,b show the zonally and annually averaged surface temperature difference between simulation GRASS and simulation FOREST. The bottom panels in Figs. 10a,b give the decomposition of this signal with respect to the four above-mentioned factors. (Note that combining linearly these different terms enables to retrieve the net biogeophysical signal.)

When considering only the surface temperature change occurring over deforested areas (Fig. 10a), it appears that conversion from forest to grassland leads to a

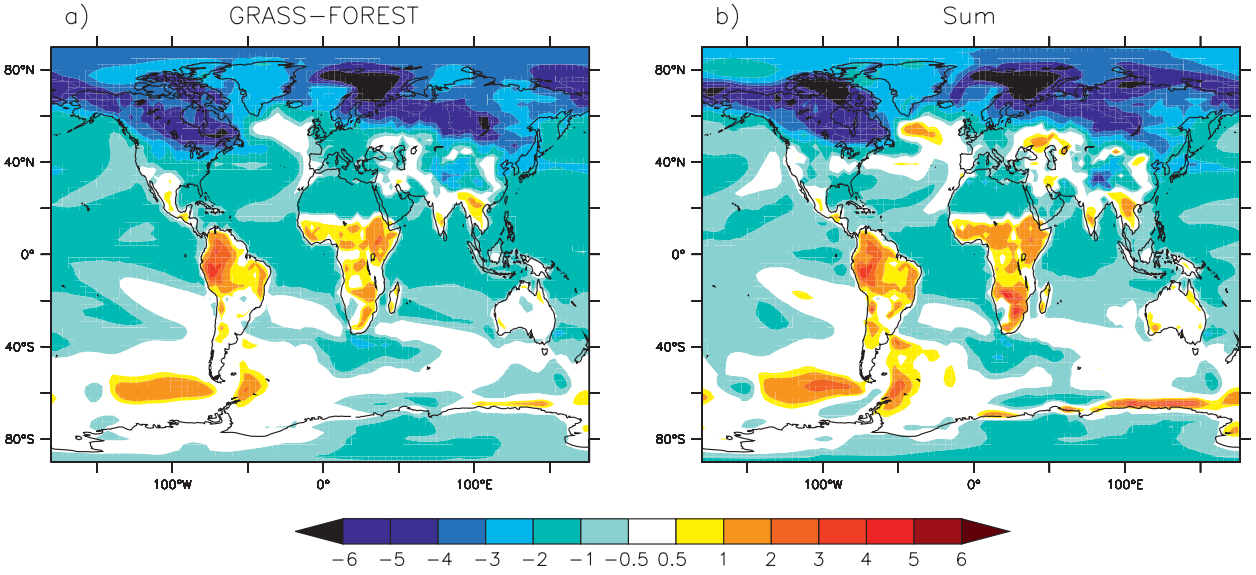

FIG. 9. Change in annual mean surface temperature (K) (a) in simulation GRASS relative to simulation FOREST and (b) reconstructed as the sum of the effects of change in albedo, evapotranspiration efficiency, and roughness.

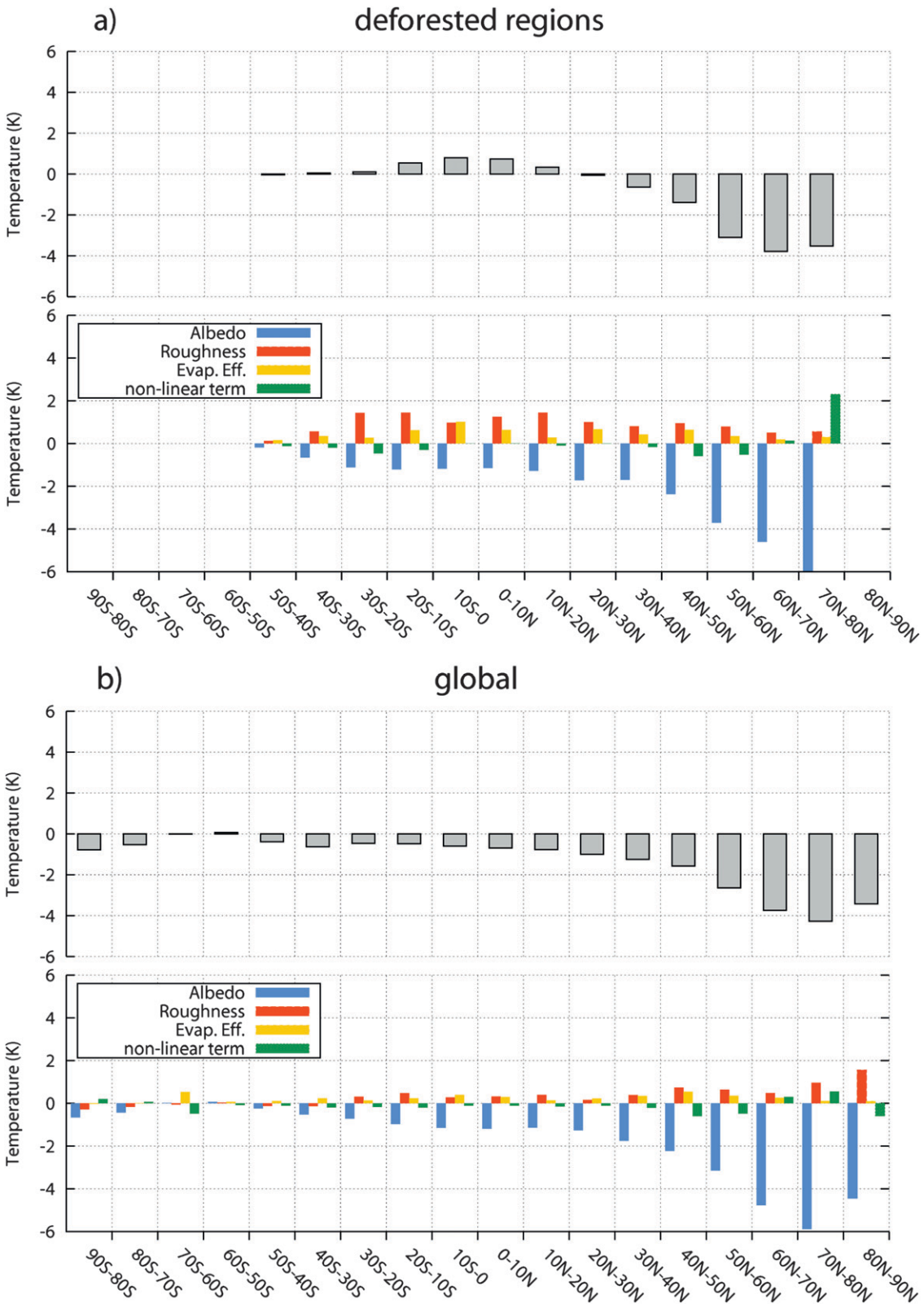

FIG. 10. Annual mean change in surface temperature zonally averaged over (a) deforested areas only and (b) both land and oceans. The bottom panel of each figure indicates the relative contribution of change in surface albedo, change in evapotranspiration efficiency, change in surface roughness, and nonlinear effects.

surface warming of 0.5–1 K in the tropics (between 20°S and 20°N). This is because the effects of evapotranspiration efficiency and surface roughness dominate the temperature signal, although albedo change partly offsets the surface warming. In contrast, beyond 30°N the net biogeophysical effect of deforestation is a cooling of climate of up to 3–4 K at highest latitudes. Indeed, the magnitude of the albedo effect increases with latitude, while the influence of evapotranspiration efficiency and surface roughness tends to vanish at high latitudes. Albedo change is thus the dominant factor in temperate and boreal regions. Between 20°N and 30°N and also beyond 20°S deforestation has no significant impact because the individual effects offset each other.

In addition to these annual mean results, we note that there are relatively few seasonal variations in the effect of deforestation (not shown). In the tropics, the individual factors and thus the net effect of deforestation remain roughly constant throughout the year. In temperate and boreal regions, the net cooling associated with deforestation is only slightly lower in summer compared to winter (−1.9 K for JJA versus −2.4 K for DJF, averaged over land beyond 30°N) because of the seasonality of evapotranspiration efficiency and surface roughness effects (as shown in Figs. 5 and 7). On the other hand, the albedo effect remains strong in summer in our experiments, thus sustaining the net cooling throughout the year. Since albedo forcing is enhanced in the presence of snow, one may expect a larger impact in winter. However, Bonan et al. (1992) already noted that the winter–spring cooling caused by boreal deforestation in a coupled ocean–atmosphere model can be perpetuated year-round because of the combination of the sea ice feedback and the thermal lag introduced by the ocean.

When considering the surface temperature change integrated over both land and ocean (Fig. 10b), the net effect of deforestation becomes a cooling at every latitudes. It can be seen on the bottom panel of Fig. 10b that this is because the albedo effect dominates the temperature signal even at low latitudes. This means that albedo change has a wider-scale influence in contrast to the other factors. Regionally, the albedo effect can be masked by the warming effect in deforested areas, but at a larger scale it dominates the temperature signal. The mechanism behind this result is explored in the next section.

d. Importance of the ocean response

Among the previous studies that examined the climatic impact of land cover change, very few have been using coupled ocean–atmosphere models. Therefore, little is known about the potential feedbacks associated with the oceanic response to perturbation of land surface parameters. Based on our experiments, we found that the ocean surface experienced a pronounced cooling in response to deforestation (see Fig. 3a).

To understand why deforestation leads to an ocean cooling, we need to examine how the perturbation due to deforestation is transferred from the land to the ocean through atmospheric processes. Figure 11 shows the global mean changes in temperature and specific humidity throughout the atmosphere for the different simulations with respect to simulation FOREST. Comparing simulation GRASS with simulation FOREST, it appears that deforestation leads globally to a tropospheric cooling (Fig. 11a). The temperature across the whole troposphere is indeed reduced by more than 1 K. Furthermore, this tropospheric cooling is associated with a decrease in water vapor content (Fig. 11b). Cooler and drier air in the troposphere, in turn, means less longwave radiation transmitted from the atmosphere to the ocean surface. Consequently, less energy is absorbed at the ocean surface, thus explaining the decrease in sea surface temperatures.

Examination of the effect of the individual surface parameters is necessary to clarify the origin of this overall response. First, focusing on evapotranspiration efficiency and surface roughness, it appears that change in these parameters only has a very limited impact on tropospheric temperatures and humidity (Figs. 11a,b). Influence of deforestation through these parameters is confined to the near-surface air and does not extend higher in the atmosphere. Consequently the associated perturbation cannot be transferred from the land to the ocean and almost no impact on ocean temperatures is observed (see Figs. 3c,d). The only parameter whose effect largely extends beyond the boundary layer is surface albedo. In fact, most of the reduction in tropospheric temperatures and humidity is related to the change in surface albedo following deforestation. Indeed, the change in tropospheric temperatures and humidity is almost identical in simulation ALB and in simulation GRASS (Figs. 11a,b). By increasing surface albedo, deforestation reduces absorption of solar energy by the surface. Consequently, less energy (both heat and radiation) can be transferred from the surface to the atmosphere, leading to a tropospheric cooling and drying, which finally leads to an ocean cooling.

This result contrasts with that obtained by (Betts 1999), who found only small changes in ocean surface temperature in a global deforestation experiment with a coupled ocean–atmosphere model. Several aspects may explain their different result. First, the vegetation perturbation they imposed (current vegetation converted to bare soil) differs from ours. Moreover, their model used flux

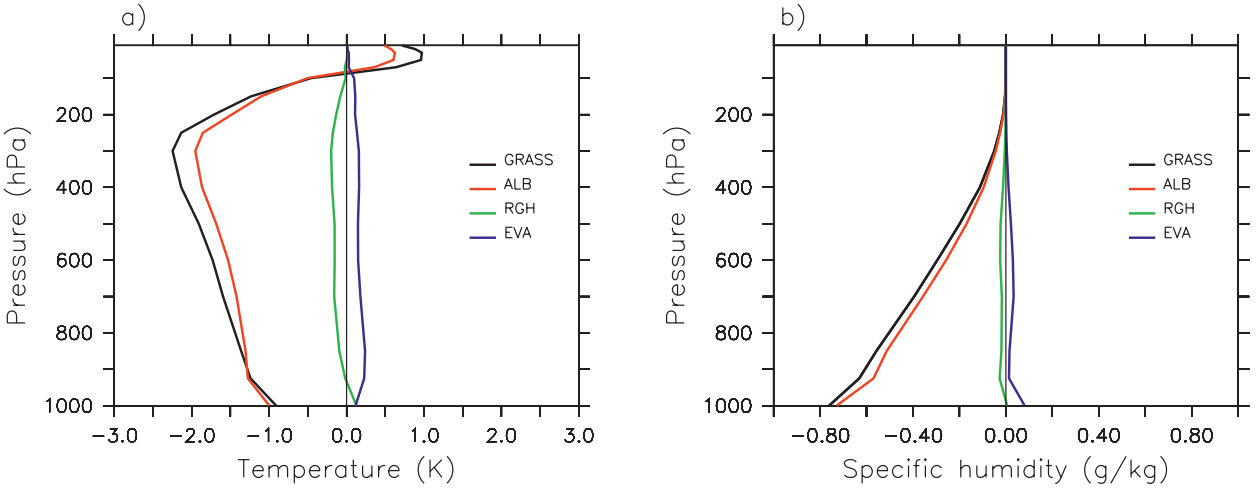

FIG. 11. Global mean change in (a) temperature and (b) specific humidity in the atmosphere for the different simulations relative to simulation FOREST.

adjustments whereas our model does not. However, the reason most likely to explain differences is that the surface albedo increase due to deforestation is compensated by a decrease in cloud cover in their experiment, thus limiting the earth's radiative imbalance. This particularly highlights the potential importance of cloud processes in the uncertainty associated with climatic impact of deforestation.

That said, our result is in agreement with several previous studies with respect to the ocean response (Bonan et al. 1992; Claussen et al. 2001; Delire et al. 2001; Ganopolski et al. 2001). For instance, using a model of intermediate complexity, Claussen et al. (2001) also found that deforestation (particularly in the tropics) can lead to an ocean cooling. Our findings thus reinforce their conclusion, but provide a different explanation concerning the underlying mechanism. Claussen et al. (2001) hypothesized that the ocean cooling arises from the reduction of evapotranspiration following deforestation (less evapotranspiration translating to less atmospheric water vapor and thus reduced atmospheric radiation down to the ocean). Instead, our experimental setup allows us to conclude that the change in surface albedo is the initial mechanism leading to the ocean cooling.

A striking feature in our experiments is that deforestation impacts climate at a large scale, in particular by cooling down the ocean surface, even though the initial perturbation is confined to land areas. Conversely, one can also expect that change in oceanic conditions may in turn feedback on the land surface temperature. To investigate this hypothesis, we perform an additional simulation with the IPSL model. This simulation has the same setup as simulation GRASS except for the ocean model, which is deactivated and replaced by prescribed sea surface temperatures and sea ice distribution. The sea surface temperatures and sea ice data are taken from the simulation FOREST, so that comparing this simulation with simulation FOREST illustrates the biogeophysical impact of deforestation under fixed oceanic conditions. The annual mean change in surface temperature, zonally averaged over land areas, is shown in Fig. 12. Experiments with calculated SSTs or with prescribed SSTs give a qualitatively similar picture in the sense that they both indicate that deforestation has a warming influence at low latitudes and a cooling influence at higher latitudes. However, the magnitude of the temperature change largely differs between the two cases. If ocean feedbacks are not taken into account, the surface warming is overestimated by more than 1 K in the tropics and the Northern Hemisphere cooling is underestimated by about 2 K. In other words, interactions with the ocean provide a positive feedback in regions where albedo change is the dominant influence. In other regions (essentially in the tropics), interactions with the ocean act as a negative feedback by dampening the temperature increase over land. Finally, a good way to illustrate the importance of the ocean coupling is to examine the averaged land surface temperature change. Considering fixed oceanic conditions, global deforestation produces an annual mean land warming of 0.5 K. Including the coupling with the ocean leads to a land temperature change of opposite sign (a land cooling of 1.1 K).

e. Radiative versus nonradiative forcings

Converting forest to grass triggers two competing effects: a cooling effect due to the increase in surface albedo and a warming effect due to both evapotranspiration

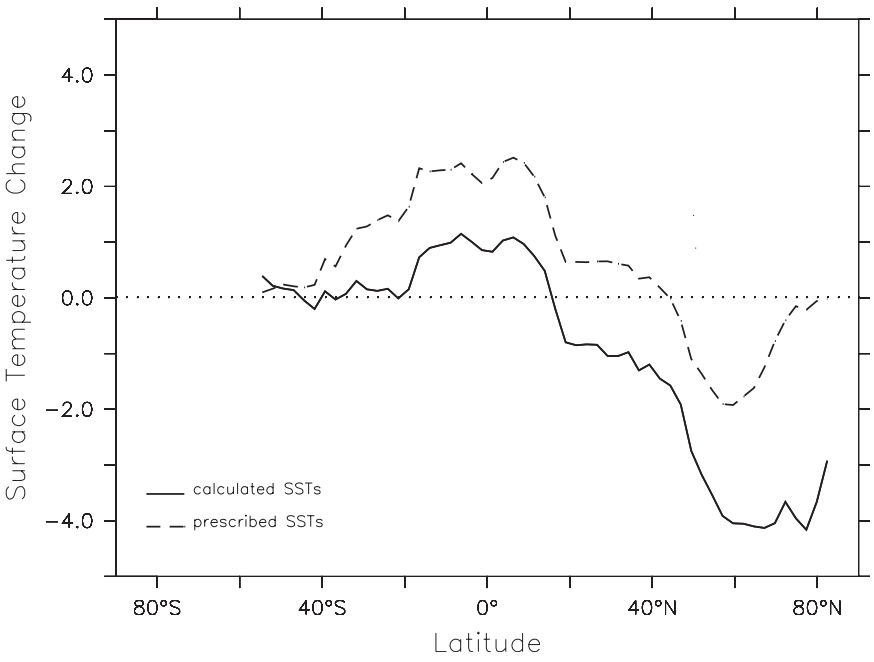

FIG. 12. Annual mean change in surface temperature zonally averaged over land in the coupled experiment (solid line) and in the experiment with prescribed SSTs (dotted line).

efficiency and surface roughness decrease. Besides their opposite sign, these two competing effects can also be opposed on the ground of their physical nature. It is known, for instance, that change in surface albedo modifies temperature by directly altering the earth's radiative balance. On the other hand, it is not clear whether change in evapotranspiration efficiency and surface roughness implies any perturbation of the earth's radiative balance. One can argue that, since these effects involve change in evapotranspiration, they can modify the water vapor content of the atmosphere and thus produce a direct radiative perturbation (Claussen et al. 2001). However, recent radiative forcing estimates (Davin et al. 2007) suggest that the radiative impact of changing evapotranspiration is likely to be small compared to the radiative forcing exerted by albedo change. Therefore, we suggest that climatic impact of deforestation through change in evapotranspiration efficiency and surface roughness is essentially a nonradiative effect.

This hypothesis can be verified by examining the change in the radiative budget at the top of the atmosphere in the different experiments. Table 1 lists the change in net radiation averaged over the first 10 years for each simulation with respect to simulation FOREST. Although it should not be viewed as an actual radiative forcing estimate, it gives a good sense of the magnitude of the radiative perturbation imposed in the experiments. Change in surface albedo produces a strong radiative imbalance of -1.27 W m^{-2} in simulation ALB relative to simulation FOREST. This imbalance has to be compensated by a temperature decrease. Interestingly, the ratio between the quasi-equilibrium surface temperature at the end of the simulation and the initial radiative imbalance (-1.36 K/-1.27 W m^{-2} = 1.07 K/W m^{-2}) is very close to the equilibrium climate sensitivity of the IPSL model deduced from CO_2 doubling experiments (around 1.2 K/W m^{-2}; Randall et al. 2007). Hence, the surface cooling is consistent with the radiative perturbation produced by albedo increase. In the case of simulations EVA and RGH, the radiative imbalance only reaches +0.02 and +0.04 W m^{-2}, respectively. Comparing these values with the temperature response (0.24 K/0.02 W m^{-2} = 12 K/W m^{-2} and 0.29 K/0.04 W m^{-2} = 7.25 K/W m^{-2}) does not reflect the actual climate sensitivity of the model. This means that the surface temperature response to change in evapotranspiration efficiency or surface roughness cannot be explained in terms of a radiative perturbation. These results demonstrate that the nature of the forcing owing to change in evapotranspiration efficiency or surface roughness is different from a classical radiative forcing perturbation. Instead, the climatic influence of these factors involves internal redistribution of energy in the climate system.

These results have strong implications for application of the radiative forcing concept. It has already been stressed that quantifying the climatic impact of land cover change through the radiative forcing framework may be misleading, in particular because nonradiative

effects of land cover change cannot be accounted for within this concept (Pielke et al. 2002; NRC 2005; Davin et al. 2007). However, the actual importance of nonradiative effects has never been explicitly quantified. Our experiments show that globally nonradiative effects (evapotranspiration efficiency and surface roughness) owing to complete deforestation warm the planet by 0.53 K (=0.24 + 0.29), thus offsetting by about 40% the cooling induced by albedo increase (−1.36 K). This implies that estimating the impact of land cover change from the radiative forcing concept can lead to overestimate the global temperature response by almost a factor of 2.

4. Conclusions

In this study we addressed the biogeophysical impact of deforestation with a fully coupled land–ocean–atmosphere GCM. We contrasted the climate of a maximally forested earth with the climate resulting from the replacement of forest by grass. Our experimental design allows us to separate the respective roles of surface albedo, evapotranspiration efficiency, and surface roughness in shaping the net biogeophysical effect of deforestation. Whereas our main focus here was on the energy budget and surface temperature, investigations of the response of the hydrological cycle will be conducted in the future.

Increase in surface albedo owing to complete deforestation has a cooling effect on climate (−1.36 K globally). On the other hand, forest removal decreases evapotranspiration efficiency and surface roughness, which warms surface climate (respectively, by 0.24 and 0.29 K globally). The magnitude of these different effects varies regionally. The cooling effect due to albedo change is stronger at high latitudes and affects both land and ocean. Conversely, the warming effect from change in evapotranspiration efficiency and surface roughness is stronger at low latitudes and does not affect the oceans.

The net biogeophysical impact of deforestation results from the competition between these effects. Globally, the albedo effect is dominant and the net biogeophysical impact of deforestation is a cooling of −1 K. This is mainly because the albedo effect spreads over the ocean, whereas the other effects do not. On continents, however, the balance between the different processes changes with latitude. In temperate and boreal zones of the Northern Hemisphere the albedo effect is stronger and deforestation thus induces a cooling, as has already been noticed in previous studies (e.g., Betts 2001; Bounoua et al. 2002). Conversely, in the tropics the net impact of deforestation is a warming because evapotranspiration efficiency and surface roughness provide the dominant influence in these regions.

This study also highlights the importance of the coupling with the ocean. Up to now, most of our knowledge concerning the impact of land cover change on climate comes from atmospheric models not coupled to an ocean model but instead assuming fixed oceanic conditions (e.g., Dickinson and Henderson-Sellers 1988; Nobre et al. 1991; Bonan 1997; Lean and Rowntree 1997; Chase et al. 2000; Gedney and Valdes 2000; Betts 2001; Bounoua et al. 2002; DeFries et al. 2002; Voldoire 2006). Implicitly, this assumption was justified be the fact that the perturbation owing to land cover change is applied to land and not to the ocean. However, our experiments show that taking into account the coupling with the ocean greatly affect the simulated response to deforestation. First, we noted that the ocean surface responds to deforestation by a cooling. Second, even the temperature change over land is strongly affected by the ocean coupling. By not taking into account the coupling with the ocean we would have concluded that the net effect of deforestation, averaged over all land areas, is a warming. By accounting for the ocean coupling, this net effect is of opposite sign. We also further demonstrated that the main parameter involved in the coupling with the ocean is surface albedo. This is because change in albedo modifies temperature and humidity in the whole troposphere, thus enabling the initially land-confined perturbation to be transferred to the ocean.

Finally, the results presented here give some insight concerning the nature of the forcing owing to land cover change. Supporting earlier hypothesis (Pielke et al. 2002; NRC 2005; Davin et al. 2007), we showed that deforestation involves two opposite types of forcing mechanisms: a radiative forcing (owing to surface albedo change) and a nonradiative forcing (owing to change in evapotranspiration efficiency and surface roughness). We quantified the relative importance of these opposite forcings in the context of our complete deforestation experiments and found that, globally, they are of similar magnitude. This result highlights the limitation of the classical radiative forcing framework in which equilibrium temperature change is viewed as a response to a radiative forcing perturbation. Land cover change can also affect equilibrium temperature through nonradiative processes. Historical deforestation took place mostly in temperate regions, and therefore radiative forcing was roughly acceptable in quantifying its effect. Future deforestation, however, is expected to take place in the tropics where nonradiative effects are dominant. Hence, using the radiative forcing framework in the context of future land cover change may lead to a misrepresentation of its impact on climate.

Acknowledgments. We are grateful to Pierre Friedlingstein and two anonymous reviewers for their useful

comments on the manuscript. Part of this research was supported by the Agence Nationale de la Recherche (ANR) through the DIVA project and by the EU funded project ENSEMBLES (GOCE-CT-2003-505539). The computing time was provided by the Commissariat à l'Énergie atomique (CEA).

REFERENCES

Alcamo, J., and Coauthors, 1994: Modeling the global society-biosphere-climate system: Part 2: Computed scenarios. *Water Air Soil Pollut.,* **76,** 37–78.

Bala, G., K. Caldeira, M. Wickett, T. J. Phillips, D. B. Lobell, C. Delire, and A. Mirin, 2007: Combined climate and carbon-cycle effects of large-scale deforestation. *Proc. Natl. Acad. Sci. USA,* **104,** 6550–6555.

Betts, R. A., 1999: Self-beneficial effects of vegetation on climate in an ocean–atmosphere general circulation model. *Geophys. Res. Lett.,* **26,** 1457–1460.

——, 2000: Offset of the potential carbon sink from boreal forestation by decreases in surface albedo. *Nature,* **408,** 187–190.

——, 2001: Biogeophysical impacts of land use on present-day climate: Near-surface temperature change and radiative forcing. *Atmos. Sci. Lett.,* **2,** 39–51, doi:10.1006/asle.2001.0037.

——, P. D. Falloon, K. K. Goldewijk, and N. Ramankutty, 2007: Biogeophysical effects of land use on climate: Model simulations of radiative forcing and large-scale temperature change. *Agric. For. Meteor.,* **142,** 216–233.

Bonan, G. B., 1997: Effects of land use on the climate of the United States. *Climatic Change,* **37,** 449–486.

——, 2008: Forests and climate change: Forcings, feedbacks, and the climate benefits of forests. *Science,* **320,** 1444–1449, doi:10.1126/science.1155121.

——, D. Pollard, and S. L. Thompson, 1992: Effects of boreal forest vegetation on global climate. *Nature,* **359,** 716–718.

Bounoua, L., R. DeFries, G. J. Collatz, P. Sellers, and H. Khan, 2002: Effects of land cover conversion on surface climate. *Climatic Change,* **52,** 29–64.

Brovkin, V., A. Ganopolski, M. Claussen, C. Kubatzki, and V. Petoukhov, 1999: Modelling climate response to historical land cover change. *Global Ecol. Biogeogr.,* **8,** 509–517.

——, and Coauthors, 2006: Biogeophysical effects of historical land cover changes simulated by six Earth system models of intermediate complexity. *Climate Dyn.,* **26,** 587–600.

Chase, T. N., R. A. Pielke, T. G. F. Kittel, R. R. Nemani, and S. W. Running, 2000: Simulated impacts of historical land cover changes on global climate in northern winter. *Climate Dyn.,* **16,** 93–105.

Claussen, M., V. Brovkin, and A. Ganopolski, 2001: Biogeophysical versus biogeochemical feedbacks of large-scale land cover change. *Geophys. Res. Lett.,* **28,** 1011–1014.

Culf, A. D., J. L. Esteves, O. Marques Filho, and H. R. da Rocha, 1996: Radiation, temperature and humidity over forest and pasture in Amazonia. *Amazonian Deforestation and Climate,* J. H. C. Gash et al., Eds., John Wiley & Sons, 175–191.

Davin, E. L., N. de Noblet-Ducoudré, and P. Friedlingstein, 2007: Impact of land cover change on surface climate: Relevance of the radiative forcing concept. *Geophys. Res. Lett.,* **34,** L13702, doi:10.1029/2007GL029678.

DeFries, R. S., L. Bounoua, and G. J. Collatz, 2002: Human modification of the landscape and surface climate in the next fifty years. *Global Change Biol.,* **8,** 438–458.

Delire, C., P. Behling, M. Coe, J. Foley, R. Jacob, J. Kutzbach, Z. Liu, and S. Vavrus, 2001: Simulated response of the atmosphere-ocean system to deforestation in the Indonesian Archipelago. *Geophys. Res. Lett.,* **28,** 2081–2084.

Dickinson, R. E., and A. Henderson-Sellers, 1988: Modeling tropical deforestation—A study of GCM land surface parametrizations. *Quart. J. Roy. Meteor. Soc.,* **114,** 439–462.

Feddema, J., K. Oleson, G. Bonan, L. Mearns, L. E. Buja, G. A. Meehl, and W. M. Washington, 2005a: The importance of land-cover change in simulating future climates. *Science,* **310,** 1674–1678.

——, ——, ——, ——, W. Washington, G. Meehl, and D. Nychka, 2005b: A comparison of a GCM response to historical anthropogenic land cover change and model sensitivity to uncertainty in present-day land cover representations. *Climate Dyn.,* **25,** 581–609.

Fichefet, T., and M. A. M. Maqueda, 1997: Sensitivity of a global sea ice model to the treatment of ice thermodynamics and dynamics. *J. Geophys. Res.,* **102** (C6), 12 609–12 646.

Ganopolski, A., V. Petoukhov, S. Rahmstorf, V. Brovkin, M. Claussen, A. Eliseev, and C. Kubatzki, 2001: Climber-2: A climate system model of intermediate complexity. Part II: Model sensitivity. *Climate Dyn.,* **17,** 735–751.

Gedney, N., and P. J. Valdes, 2000: The effect of Amazonian deforestation on the Northern Hemisphere circulation and climate. *Geophys. Res. Lett.,* **27,** 3053–3056.

Gibbard, S., K. Caldeira, G. Bala, T. J. Phillips, and M. Wickett, 2005: Climate effects of global land cover change. *Geophys. Res. Lett.,* **32,** L23705, doi:10.1029/2005GL024550.

Goldewijk, K. K., 2001: Estimating global land use change over the past 300 years: The HYDE database. *Global Biogeochem. Cycles,* **15,** 417–433.

Govindasamy, B., P. B. Duffy, and K. Caldeira, 2001: Land use changes and Northern Hemisphere cooling. *Geophys. Res. Lett.,* **28,** 291–294.

Henderson-Sellers, A., R. E. Dickinson, T. B. Durbidge, P. J. Kennedy, K. Mcguffie, and A. J. Pitman, 1993: Tropical deforestation–modeling local-scale to regional-scale climate change. *J. Geophys. Res.,* **98** (D4), 7289–7315.

Hourdin, F., and Coauthors, 2006: The LMDZ4 general circulation model: Climate performance and sensitivity to parametrized physics with emphasis on tropical convection. *Climate Dyn.,* **27,** 787–813.

Krinner, G., and Coauthors, 2005: A dynamic global vegetation model for studies of the coupled atmosphere-biosphere system. *Global Biogeochem. Cycles,* **19,** GB1015, doi:10.1029/2003GB002199.

Lean, J., and D. A. Warrilow, 1989: Simulation of the regional climatic impact of Amazon deforestation. *Nature,* **342,** 411–413.

——, and P. R. Rowntree, 1997: Understanding the sensitivity of a GCM simulation of Amazonian deforestation to the specification of vegetation and soil characteristics. *J. Climate,* **10,** 1216–1235.

——, C. B. Bunton, C. A. Nobre, and P. R. Rowntree, 1996: The simulated impact of Amazonian deforestation on climate using measured ABRACOS vegetation characteristics. *Amazonian Deforestation and Climate,* J. H. C. Gash et al., Eds., John Wiley & Sons, 549–576.

Loveland, T. R., B. C. Reed, J. F. Brown, D. O. Ohlen, Z. Zhu, L. Yang, and J. W. Merchant, 2000: Development of a global land cover characteristics database and IGBP DISCover from 1 km AVHRR data. *Int. J. Remote Sens.,* **21,** 1303–1330.

Madec, G., P. Delecluse, M. Imbard, and M. Lévy, 1998: OPA 8.1, Ocean General Circulation Model Reference Manual. Note du Pôle de Modélisation 11, 91 pp.

Marti, O., and Coauthors, 2005: The new IPSL climate system model: IPSL-CM4. Note du Pôle de Modélisation 26, 86 pp.

Nabuurs, G., and Coauthors, 2007: Forestry. *Climate Change 2007: Mitigation,* B. Metz et al., Eds., Cambridge University Press, 541–584.

Nobre, C. A., P. J. Sellers, and J. Shukla, 1991: Amazonian deforestation and regional climate change. *J. Climate,* **4,** 957–988.

NRC, 2005: *Radiative Forcing of Climate Change: Expanding the Concept and Addressing Uncertainties*. The National Academies Press, 207 pp.

Pielke, R. A., G. Marland, R. A. Betts, T. N. Chase, J. L. Eastman, J. O. Niles, D. D. S. Niyogi, and S. W. Running, 2002: The influence of land-use change and landscape dynamics on the climate system: Relevance to climate-change policy beyond the radiative effect of greenhouse gases. *Philos. Trans. Roy. Soc. London,* **A360,** 1705–1719.

Ramankutty, N., and J. A. Foley, 1999: Estimating historical changes in global land cover: Croplands from 1700 to 1992. *Global Biogeochem. Cycles,* **13,** 997–1027.

Randall, D., and Coauthors, 2007: Climate models and their evaluation. *Climate Change 2007: The Physical Science Basis,* S. Solomon et al., Eds., Cambridge University Press, 589–662.

Sitch, S., and Coauthors, 2003: Evaluation of ecosystem dynamics, plant geography and terrestrial carbon cycling in the LPJ dynamic global vegetation model. *Global Change Biol.,* **9,** 161–185.

Snyder, P., C. Delire, and J. Foley, 2004: Evaluating the influence of different vegetation biomes on the global climate. *Climate Dyn.,* **23,** 279–302, doi:10.1007/s00382-004-0430-0.

Solomon, S., D. Qin, M. Manning, M. Marquis, K. Averyt, M. M. B. Tignor, H. L. Miller, and Z. Chen, Eds., 2007: *Climate Change 2007: The Physical Science Basis*. Cambridge University Press, 996 pp.

Sud, Y. C., J. Shukla, and Y. Mintz, 1988: Influence of land surface roughness on atmospheric circulation and precipitation: A sensitivity study with a general circulation model. *J. Appl. Meteor.,* **27,** 1036–1054.

Voldoire, A., 2006: Quantifying the impact of future land-use changes against increases in GHG concentrations. *Geophys. Res. Lett.,* **33,** L04701, doi:10.1029/2005GL024354.

von Randow, C., and Coauthors, 2004: Comparative measurements and seasonal variations in energy and carbon exchange over forest and pasture in south west Amazonia. *Theor. Appl. Climatol.,* **78,** 5–26.